ELSEVIER

Biophysical Chemistry 111 (2004) 53–61

Biophysical Chemistry

www.elsevier.com/locate/bpc

Proton dependence of tobacco mosaic virus dissociation by pressure

Jose L.R. Santos, Jose A.C. Bispo, Gustavo F. Landini, Carlos F.S. Bonafe*

Laboratório de Termodinâmica de Proteínas, Departamento de Bioquímica, Instituto de Biologia, Universidade Estadual de Campinas (UNICAMP), CP 6109, Campinas, SP, CEP 13083-970, Brazil

Received in revised form 15 April 2004; accepted 16 April 2004
Available online 8 May 2004

Abstract

Tobacco mosaic virus (TMV) is an intensely studied model of viruses. This paper reports an investigation into the dissociation of TMV by pH and pressure up to 220 MPa. The viral solution (0.25 mg/ml) incubated at 277 K showed a significant decrease in light scattering with increasing pH, suggesting dissociation. This observation was confirmed by HPLC gel filtration and electron microscopy. The calculated volume change of dissociation (ΔV) decreased (absolute value) from -49.7 ml/mol of subunit at pH 3.8 to -21.7 ml/mol of subunit at pH 9.0. The decrease from pH 9.0 to 3.8 caused a stabilization of 14.1 kJ/mol of TMV subunit. The estimated proton release calculated from pressure-induced dissociation curves was 0.584 mol H^+/mol of TMV subunit. These results suggest that the degree of virus inactivation by pressure and the immunogenicity of the inactivated structures can be optimized by modulating the surrounding pH.

Keywords: Tobacco mosaic virus; Pressure-induced dissociation; Virus dissociation

1. Introduction

Tobacco mosaic virus (TMV), a rod-shaped virus with 2130 protein subunits of 17.5 kDa and a 6.4 kb RNA molecule, has been extensively investigated as a model of viral assembly. The use of intact virus provides a unique system for investigations of viral stability because of the high number of protein–RNA interactions present during TMV uncoating [1–3]. Investigations of TMV destabilization by alkaline solutions have shown a polar disassembly from 5′ to 3′ RNA and the presence of several intermediates [4–10]. The dissociation of TMV at pH values between pH 9.5 and 10.5 followed by separation of the products in agarose gels has revealed a predominance of several distinct, stripped virus particles corresponding to about 93%, 68%, 61%, 39%, 31%, 24% and 16% of the total virus length (~300 nm) [11]. Other investigations using different methods have reported similar intermediates, with some variation in number and size [10–12]. The role of protons in the mechanisms of subunit association during the self-assembly of TMV coat proteins has also been investigated [13–15].

The use of low temperatures, high pressure and chemical agents to produce significant disassembly of TMV particles provides a means of studying the thermodynamics of the uncoating process and its modulation by changes in pH. This approach also allows comparison with the behavior of TMV coat proteins already extensively described in the literature.

Experiments done by Blowers and Wilson [16] using urea to promote the disassembly of TMV particles have shown that protein dissociation occurs predominantly from the 5′ to the 3′-end of the RNA molecule, in a manner similar to that observed for alkaline dissociation. In other viruses, such as cowpea mosaic virus, a high hydrostatic pressure in combination with urea has been used to show that the RNA molecule stabilized the virus particle and increased the reversibility of pressure-induced denaturation [17].

Studies of other virus interactions indicate that the subunit assembly is facilitated by specific interactions between the protein subunits and an internal RNA sequence [18–21]. In TMV, this RNA sequence, known as the ‘‘assembly origin’’, allows the nucleation necessary for further elongation [22]. A consequence of this property is that modifications in the RNA conformation and the occurrence of mutations and changes in the external conditions may affect the initiation of coating, as well as the velocity of aggregation through changes in the protein–RNA interac-

* Corresponding author. Tel.: +55-19-3788-6135; fax: +55-19-3788-6129.
E-mail address: bonafe@unicamp.br (C.F.S. Bonafe).

0301-4622/$ - see front matter © 2004 Elsevier B.V. All rights reserved.
doi:10.1016/j.bpc.2004.04.003

tions, predominantly at the assembly origin. Extensive experimental evidence indicates that TMV assembly involves nucleation and fast elongation through the incorporation of a 20 S disk aggregate (38–42 coat protein subunits) at the 5′-terminus of the RNA, and slower elongation of smaller or single-coat proteins toward the 3′-terminus [23,24].

We recently described some thermodynamic aspects of TMV dissociation by high hydrostatic pressure under several conditions, including subzero temperatures and in the presence of urea [25]. The dissociation of TMV particles was detected as a decrease in the intensity of light scattering by the virus in solution. The occurrence of denatured structures was in turn discriminated by the red shift of the fluorescence emission spectrum. These results indicated no significant denaturation when pressure-induced dissociation of the virus capsid occurred at low temperature and in the absence of urea. Significant dissociation was observed at subdenaturating concentrations of urea (2.5 M). Marked denaturation was seen only at high urea concentrations or at subdenaturating concentrations of urea in combination with pressure.

In this work, we have extended our study of TMV particles by investigating the modifications in virus properties induced by pH and high hydrostatic pressure. The occurrence of denaturation under these conditions was analyzed using lifetime measurements and fluorescence emission spectra. The methodology used to characterize the dissociation process provides the first quantitative analysis of the effect of protons on the assembly of the TMV particle and allows an estimate of the energy and volume changes at each pH. These observations, and the analysis of factors such as the binding of urea at distinct pH values, provide further insights into the structural changes that modify the protein–protein and protein–RNA interactions during TMV uncoating under specific surrounding conditions.

2. Materials and methods

2.1. Chemicals

All reagents were of analytical grade. Distilled water was filtered and deionized through a Millipore water purification system (18 MΩ resistance). The experiments were done at 4 °C with 50 mM acetate buffer for pH 4.2 to 5.5, 50 mM Bis–Tris–propane buffer for pH 6.0 and 6.5, and 50 mM Tris–HCl buffer for pH 7.0 to 9.0. The pH of the solutions was adjusted at the temperature at which the experiments were done. The Bis–Tris–propane and Tris chloride buffers were chosen because they showed negligible change in pH over the pressure range studied. The pH of the acetate buffer was corrected by subtracting 0.4 pH units from the adjusted pH over the pressure range of 150–220 MPa [26].

2.2. TMV purification

The virus was isolated from Turkish tobacco plants infected with the common strain of the virus. The virus was purified as described by Asselin and Zaitlin [27].

2.3. Light scattering and fluorescence under pressure

The high-pressure system has been described elsewhere [28]. An ISS model HP high-pressure cell with sapphire windows connected to a pressure generator (HIP) was used. Light scattering at 340 nm was recorded in an Edinburgh FL 900 spectrofluorometer and was measured at an angle of 90° relative to the incident light using the same wavelength for the excitation and emission monochromators. The intensity of light scattering by native TMV under the conditions described here was positively correlated with TMV concentrations up to 1.0 mg of virus/ml (data not shown). Because the experiments were done at TMV concentrations considerably less than 1 mg/ml, we estimated the average molecular weight based on the intensity of light scattering (equation 17–32 in Ref. [29]) at pressure p, S_p, and calculated the degree of dissociation (α) as

$$\alpha_p = (S_i - S_p)/(S_i - S_f) \quad (1)$$

where S_f and S_i are the intensities of light scattering for the dissociated and associated forms, respectively. The fluorescence data were obtained at an excitation wavelength of 285 nm and an emission of 300–400 nm.

The pressure system was automated and controlled by software denominated "Automa" written in Delphi 5.0 language and was compatible with Windows. A computer controlled a series of devices, including (1) a servomotor connected to an induction motor that was coupled to the pressure generator, (2) the fluorometer monochromators for excitation and emission, and (3) the step motors for the excitation and emission slits. The software received information from a pressure gauge via an analogic interface connected to a 14-bit analogic–digital board that allowed the control of pressure in real time, while data from the photodetectors were obtained via an RS232 serial port. All data were processed in ASCII format and displayed on x–y plots. This automation allowed the experiments to be run using preprogrammed pressure values at given incubation times. The fluorescence and light scattering measurements at each pressure were also obtained by programmed control of the monochromators and adjustment of the excitation and emission slits. The latter adjustment was necessary because the light scattering signal was much more intense than the fluorescence signal, and therefore needed to be collected with narrower slits.

2.4. Lifetime measurements

For these experiments, the samples were excited at 285 nm with an H_2-filled F900 flash lamp at a gas pressure of

0.4 bar and a pulse frequency of 40 kHz. The emission was analyzed at 320 nm in a model FS900 spectrofluorometer (Edinburgh Instruments). Time-resolved fluorescence decays were recorded and analyzed using software provided by Edinburgh Instruments.

2.5. Gel filtration

Size exclusion HPLC was done with a Shimadzu HPLC system. A prepacked SynChropack GPC 1000 column (250 × 4.6 mm, i.d.) (SynChrom, Linden, IN), was used for gel filtration. Elution of the samples was monitored by absorption at 280 nm. The void volume (V_0) of the column was measured with TMV before the application of pressure and the total volume (V_t) with a solution of human albumin. Extracellular hemoglobin (3300 kDa) from the annelid *Glossoscolex paulistus* [30] was used as a molecular mass standard in the presence of 0.1 M calcium chloride.

2.6. Electron microscopy

Transmission electron microscopy was done in a Leo-902 microscope. Negative staining was done with 1% uranyl acetate. When mentioned, the samples were fixed with 0.5% glutaraldehyde solution prior to negative staining. The samples fixed under pressure were prepared as described by Silva and Weber [31], and the respective controls were fixed at atmospheric pressure or after pressure using the same procedure. The method of fixation consisted of a bottle-shaped sample cell with two adjacent compartments, one for the sample and one for the glutaraldehyde solution. The chambers were separated by a vertical partition that did not reach the neck of the bottle. Dodecane was used to complete the volume of the cell followed by sealing with a compressible plastic cap. During the experiment, the TMV sample was incubated at high pressure and, at a given time interval, the sample was fixed by inverting and shaking the chamber for about 10 min.

2.7. Theoretical considerations

The participation of protons in virus dissociation into its subunits and genetic material [25] can be expressed as follows

$$(P_{2130}N) \overset{K^0_{atm}}{\longleftrightarrow} 2130P + N + \upsilon_D H^+ \tag{2}$$

where P is the protein subunit, N the genetic material (in this case, RNA), $P_{2130}N$ is the virus molecule, K^0_{atm} corresponds to the equilibrium constant of virus dissociation under reference conditions of atmospheric pressure and pH = 0, and υ_D is the total number of protons released or absorbed during dissociation. Because this equilibrium is likely to have several intermediate forms that probably correspond to the "stripped virus particles" mentioned above (e.g., Ref. [11]), the present considerations will be restricted to an equilibrium involving complete dissociation.

The introduction of protons in this equation is important to explain the pH dependence of this process. Thus, if the exposure of a subunit–subunit interface to the solvent modifies the interactions of residues during protein dissociation, the average pK of the amino acids affected should change, thereby generating a net proton release ($\upsilon_D > 0$) or absorption ($\upsilon_D < 0$) or even an apparent proton independence ($\upsilon_D = 0$).

The corresponding equilibrium relationship for Eq. (2) is

$$K^0_{atm} = \frac{[P]^{2130}[N][H^+]^{\upsilon_L}}{[P_{2130}N]} \tag{3}$$

This equation can be rewritten to show the behavior expected for the species at pH values other than pH = 0. Thus,

$$K^{pH}_{atm} = \frac{K^0_{atm}}{[H^+]^{\upsilon_D}} = \frac{[P]^{2130}_{pH}[N]_{pH}}{[P_{2130}N]_{pH}} \tag{4}$$

and

$$\begin{aligned} \Delta G^{pH}_{atm} &= \Delta G^0_{atm} + \upsilon_D RT \ln[H^+] \\ &= \Delta G^0_{atm} - 2.303 \upsilon_D RT\, pH \end{aligned} \tag{5}$$

where K^{pH}_{atm} is the equilibrium constant of dissociation at a given pH and atmospheric pressure, ΔG^{pH}_{atm} is the respective Gibbs free energy change of dissociation, R is the gas constant, T is the absolute temperature and ΔG^0_{atm} is the corresponding energy change of dissociation at pH = 0. The derivative form of Eq. (5) is equivalent to Eq. (20a) of Chu et al. [32] used to analyze the proton effect on hemoglobin.

The relationship that correlates this dissociation constant with the experimental pressure can be obtained based on the volume change of dissociation, ΔV [33], which gives

$$\Delta G^{pH}_p = \Delta G^{pH}_{atm} + p\Delta V \tag{6}$$

where ΔG^{pH}_p is the Gibbs free energy of dissociation at a specified pH and pressure p.

The equilibrium constant of dissociation derived from Eq. (6) corresponds to

$$K^{pH}_p = K^{pH}_{atm} \exp\left(\frac{-p\Delta V}{RT}\right) = \frac{[P]^{2130}_{pH,p}[N]_{pH,p}}{[P_{2130}N]_{pH,p}} \tag{7}$$

The presence of pH and p in the equilibrium constant of dissociation, K^{pH}_p, and in the concentrations of species on the right side of Eq. (7) indicates that these parameters are pH- and pressure-dependent. Eq. (7) rewritten in terms of the degree of dissociation, α, i.e., the ratio between the amount of virus that dissociates relative to the total amount

of virus, allows direct correlation with the experimental data [25], as follows

$$K_p^{\mathrm{pH}} = K_{\mathrm{atm}}^{\mathrm{pH}} \exp\left(\frac{-p\Delta V}{RT}\right) = \frac{2130^{2130} C^{2130} \alpha^{2131}}{(1-\alpha)} \quad (8)$$

where C is the total virus concentration and α is the degree of dissociation observed at each pH and pressure. The logarithmic form yields the linear relationships

$$\ln K_p^{\mathrm{pH}} = \ln K_{\mathrm{atm}}^{\mathrm{pH}} - \frac{p\ \Delta V}{RT} \quad (9)$$

$$= 2130\ \ln\ 2130 + 2130\ \ln\ C + 2131\ \ln\ \alpha - \ln(1-\alpha)$$

Note that, here, we considered $[P]=2130\alpha C$, $[N]=\alpha C$ and $[P_{2130}N]=(1-\alpha)C$. A plot of $\ln K_p^{\mathrm{pH}}$ versus p furnishes a straight line, the linear and angular coefficients of which are given by Eq. (9), and yields values for $K_{\mathrm{atm}}^{\mathrm{pH}}$ that can be used to calculate the values of $\Delta G_{\mathrm{atm}}^{\mathrm{pH}}$ and ΔV. The applicability and the limitations of this approach are discussed below.

3. Results

An initial analysis of TMV organization by electron microscopy showed that the number of associated TMV particles was much higher at pH 4.2 than at pH 9.0 (Fig. 1). At high pH, the particles were shorter than for native TMV. These results indicated an increase in the degree of dissociation with increasing pH, which implied a $\upsilon_D>0$ in Eq. (5).

To quantify this parameter, the light scattering by TMV was examined at various pressures and pH values (Fig. 2). The higher intensity of light scattering at low pH and atmospheric pressure indicated greater stability of the TMV particles. A shift from pH 3.8 to 9.0 resulted in a significant decrease in light scattering which was particularly marked at pH>7.0. At higher pressures (up to 220 MPa), there was a significant decrease in the intensity of light scattering to a level which was similar to that of the buffer solution. A return to atmospheric conditions after high pressure showed that the dissociated protein species produced stable structures with a reduced tendency to associate into the native TMV particle (Fig. 2, open symbols).

The gel filtration results obtained at different pressures and pH confirmed the significant dissociation caused by high pressure (Fig. 3). At low pH values and atmospheric conditions, the TMV eluted at the exclusion volume (V_0) of the column, while at alkaline pH, the elution profile corresponded to more dissociated species. Incubation under pressure significantly increased the number of dissociated forms at high pH.

Electron microscopy of TMV fixed under 220 MPa at pH 6.5 and 8.0 and then returned to atmospheric pressure showed shorter particles at high pressure. At both pH values, the dissociated protein species showed a reduced tendency to associate after incubation under pressure, despite the increase in particle size at atmospheric pressure (data not shown). These results indicated the formation of dissociated structures with low subunit affinities but some stability.

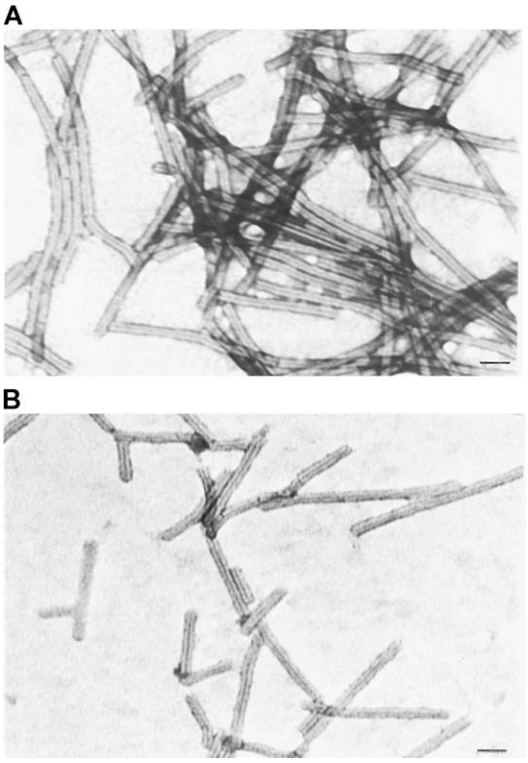

Fig. 1. Transmission electron microscopy of TMV at different pH values. TMV (0.25 mg/ml) was incubated in 50 mM buffer solutions for 24 h at (A) pH 4.2 in sodium acetate and (B) pH 9.0 in Tris–HCl. Negative staining was done with 1% uranyl acetate. Bar = 50 nm.

The corresponding degree of dissociation (α) obtained from Eq. (1) applied to the data in Fig. 2 is shown in Fig. 4A. Here, α was considered to be zero (0) for the TMV solution at pH 4.2, at which there was a greater intensity of light scattering, and $\alpha = 1$ at pH 9.0 and 220 MPa, at which the light scattering was of lower intensity, similar to the scattering seen with buffer. Fig. 4A clearly shows the increase in the degree of dissociation with increasing pH and pressure. At atmospheric pressure and pH 9.0, the TMV solution already showed partial dissociation (~47%) of the virus. Decreasing the pH increased the subunit affinity and reduced the degree of dissociation to about 10% at pH 6.5. In this case, the proton effect reduced the span of the pressure dissociation curve with decreasing pH. This behavior is characteristic of a heterogeneous population of protein species in solution and suggests that distinct virus structures subjected to dissociation should predominate at low and high pH values [30,34]. Fig. 4A and Eq. (6) also indicate that an increase in pressure reduced the Gibbs free energy of TMV dissociation, which implies a negative ΔV.

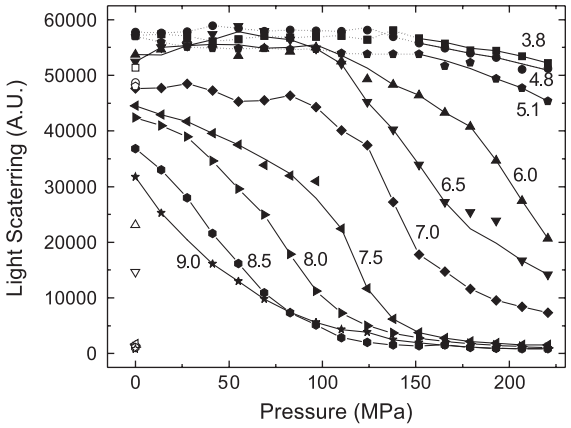

Fig. 2. Effect of pressure on TMV dissociation at different pH values. The TMV solution (0.25 mg/ml) was incubated in the following buffers (all 50 mM): sodium acetate (pH 3.8, 4.8 and 5.1 at 150 to 220 MPa, previously adjusted at atmospheric pressure to 4.2, 5.2 and 5.5, respectively, see Materials and methods), Bis–Tris propane (pH 6.0 and 6.5) and Tris–HCl (pH 7.0 to 9.0). The dashed lines, which correspond to the lower part of the curves with acetate buffer, represent a region of pH higher than that indicated in each curve. All measurements were done at a temperature of 277 K. The light scattering was measured after a 16 min incubation at each pressure value (A.U.: arbitrary units). Excitation was at 340 nm and emission at 337 to 343 nm. The total length of exposure to pressure was about 4.5 h. The open symbols correspond to data obtained 16 min after the return from 220 MPa to atmospheric pressure. Further measurements after up to 2 h showed no change in the light scattering measurements. The experiments were done in triplicate and the standard deviations were smaller than the symbols.

To determine some important quantitative parameters associated with the modifications in TMV during dissociation, we used the plot of ln K_p^{pH} versus pressure shown in Fig. 4B. As mentioned above, ΔG_{atm}^{pH} and ΔV can be estimated from the linear and angular coefficients of the fitting in Fig. 4B by using Eq. (9) at each pH. As shown in Fig. 5, ΔG_{atm}^{pH} decreased from 88.49 MJ at pH 3.8 to 58.43 MJ at pH 9.0 (Fig. 5). Thus, the decrease from pH 9.0 to 3.8 stabilized the virus particle by 30.06 MJ, corresponding to 14.1 kJ/mol of subunit. To extend the analysis of the pH dependence of TMV dissociation, we used Eq. (5) to obtain a linear fitting of the results obtained for ΔG_{atm}^{pH} versus pH, as shown in Fig. 5. The linear coefficient furnished a value of ΔG_{atm}^{0} equal to 119.43 MJ, whereas the angular coefficient yielded υ_D equal to 1246 mol of H^+/mol of virus particle, or 0.584 mol of H^+/mol of TMV subunit. The respective volume change of dissociation (Fig. 5, inset) provided additional important information on the process of dissociation. In this figure, the absolute ΔV values decreased from -49.7 to -21.7 ml/mol of subunit at pH 3.8 and 9.0, respectively. These results for the ΔV values indicated that intermediate virus structures with distinct states of aggregation were formed in solution to generate the ΔV decrease and accounted for the heterogeneous character of the sample.

To investigate whether the structures formed in solution suffered concomitant denaturation under the conditions used, we examined the fluorescence emission spectrum at various pH and pressure values (Fig. 6A). At pH 9.0 and 220 MPa, and at pH 4.2 and atmospheric pressure, there was no significant red shift in the fluorescence emission spectra (lines a and b), thus indicating negligible denaturation. Intermediate conditions of pressure and pH resulted in fluorescence spectra between these extreme values and no observable red shift in fluorescence (not shown). In contrast, the presence of 4 M urea at atmospheric pressure and pH 7.5 resulted in a very significant red shift of 2600 cm^{-1} (line c). The inset in Fig. 6A, which corresponds to the fluorescence spectra of Fig. 6A normalized relative to the maximum intensity, clearly shows the red shift induced by urea. These data were similar to those previously obtained for TMV particles [25] and indicated a lack of denaturation, even at the extreme pH values used.

The dynamic fluorescence of TMV at different pH values was determined in order to analyze the environment around tryptophans under these conditions. Fig. 6B shows a continuous increase in the measured lifetime with increasing pH at atmospheric pressure and at 220 MPa. The average change in the tryptophan environment relative to the increase in lifetime was from 2.88 to 3.51 ns at pH 4.2 and pH 9.0, respectively. At 220 MPa, these lifetime values increased from 2.90 to 4.30 ns over

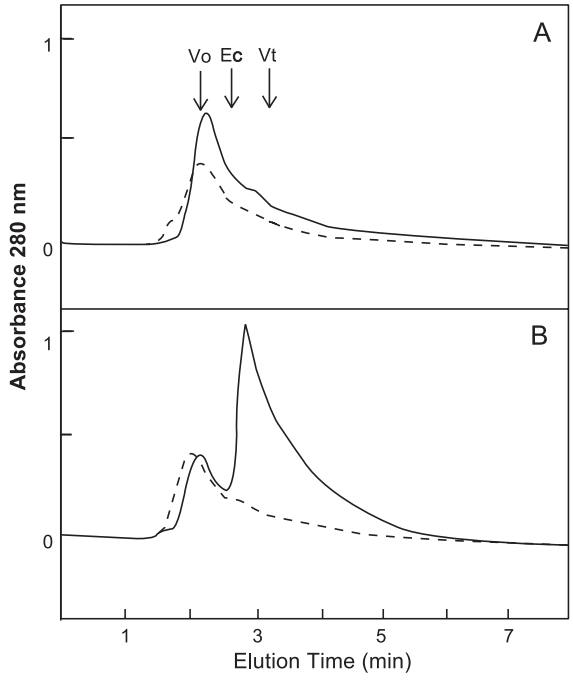

Fig. 3. Gel filtration HPLC analysis (GPC1000 column) of TMV dissociated by pressure at different pH values. A volume of 100 μl of TMV (0.25 mg/ml) was injected and eluted at a rate flow of 0.3 ml/min. Dashed line: TMV at atmospheric pressure. Continuous line: TMV after 100 min at 220 MPa. (A) pH 6.5, in 50 mM Bis–Tris–propane buffer, and (B) pH 8.0 in 50 mM Tris–HCl buffer. V_0 and V_t are the void volume and final volume, respectively, and Ec is the elution point of extracellular hemoglobin (3300 kDa) from *G. paulistus* [30].

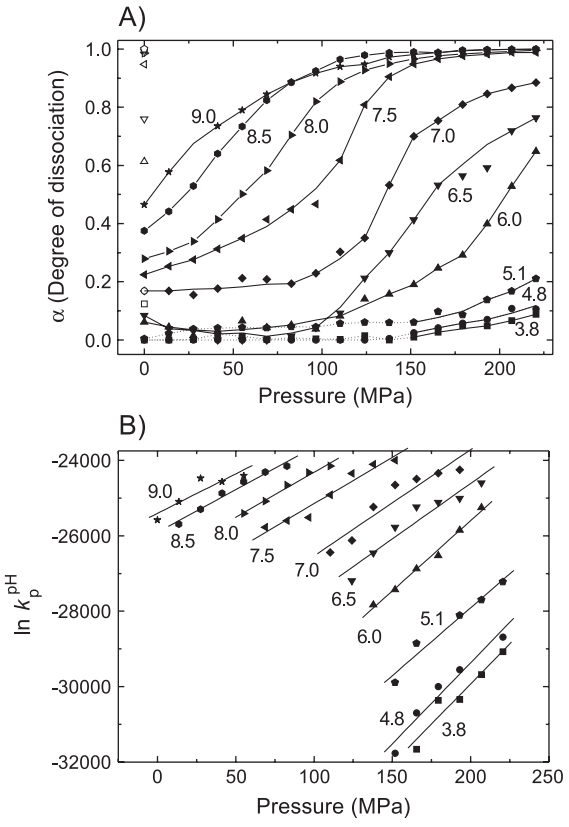

Fig. 4. (A) Degree of dissociation based on the light scattering data shown in Fig. 2 and Eq. (1). (B) Plot of ln K_p^{pH} versus pressure, where ln $K_p^{pH} = 2130 \ln 2130 + 2130 \ln C + 2131 \ln \alpha - \ln(1-\alpha)$. The symbols, solid lines and dashed lines represent the experimental results obtained under the conditions described in Fig. 2. The straight lines are the corresponding linear fits of these data at each pH.

approximately the same pH range, whereas in the presence of 4 M urea and at atmospheric pressure, the values increased from 3.16 to 7.67 ns.

4. Discussion

The dissociation experiments at different pH values and pressure indicated that, during subunit disassembly, the virus particles underwent structural changes in their subunits that led to a net release of protons. An alkaline pH facilitated dissociation by reducing the observed subunit affinity (ΔG_{atm}^{pH}). A similar pH dependence observed in several processes involving protein aggregates, including the dissociation of hemocyanin [35] and the dissociation and oxygenation of human hemoglobin [32], indicates that protons play an important role in the regulation of protein function and dynamics by modifying the predominant structures in solution. Other modulators, e.g., calcium ions, exert a significant effect on the stabilization of multiprotein assemblies, such as hemocyanin and annelid extracellular hemoglobin, and induce reassociation in pressure-dissociated molecules [35,36].

To quantify the intensity of these modifications for protons in TMV dissociation, the results obtained for the plot of ΔG_{atm}^{pH} versus pH were described using a linear model based on a single virus structure subject to dissociation. However, the experimental data showed a biphasic response, which suggested at least two distinct viral structures or states of aggregation, with each predominating at distinct extremes of pH (Fig. 5). This hypothesis was reinforced by the changes observed in the ΔV values. In this context, the number of protons released upon dissociation (0.584 mol of H^+/mol of TMV subunit) should be considered as an average value between the acid and alkaline sides. Such behavior has been observed in several systems and provides clues about the formation of dissociated structures or denaturated protein states [30,34]. An estimation of the proton release in the two phases based on the distinct angular coefficients at low and high pH (dashed lines, Fig. 5) yielded 0.643 and 0.248 mol H^+/mol of subunit under acidic and alkaline conditions, respectively. Although dissociation of the virus can be analyzed by considering more than two structural species in solution, this approach is limited by the difficulty in interpreting the light scattering for the average particle size at each pressure. Hence, a two-state process is still the simplest approach for this analysis.

Weber [37] proposed mechanisms to incorporate other protein forms in the dissociation of high protein aggregates by considering that water molecules in contact with the dissociated species would change the species' structures by interacting with hydrophobic regions. This in turn would lead to the appearance of new protein structures with low subunit affinities. The formation of these structures would be controlled by a process that would take into account the

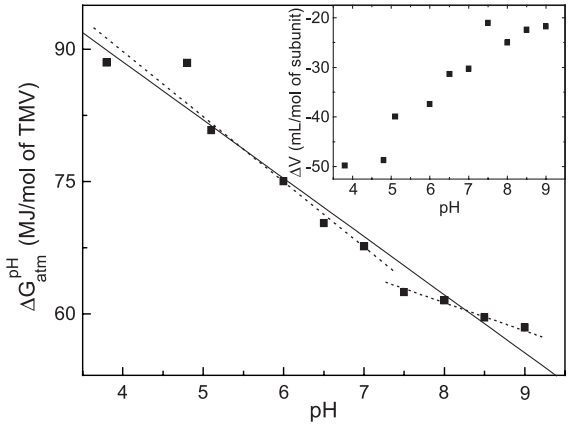

Fig. 5. Effect of pH on the Gibbs free energy of TMV dissociation, ΔG_{atm}^{pH}. These results were obtained from the linear fitting shown in Fig. 4B as applied to Eq. (9). The dashed lines correspond to the linear fits of the two pH ranges, 3.8 to 7.0 and 7.5 to 9.0. Inset: Volume change of dissociation at different pH values. The corresponding virus concentration in Eq. (9) that allowed an estimate of ΔG_{atm}^{pH} values to be obtained from the linear coefficient of the fitted curves in Fig. 4B was 0.25 mg/ml (corresponding to $C = 0.625 \ \infty$M). The gas constant used to calculate the ΔV values was $R = 8.314 \times 10^{-6}$ MJ/mol/K. The temperature of the solutions analyzed was 277 K.

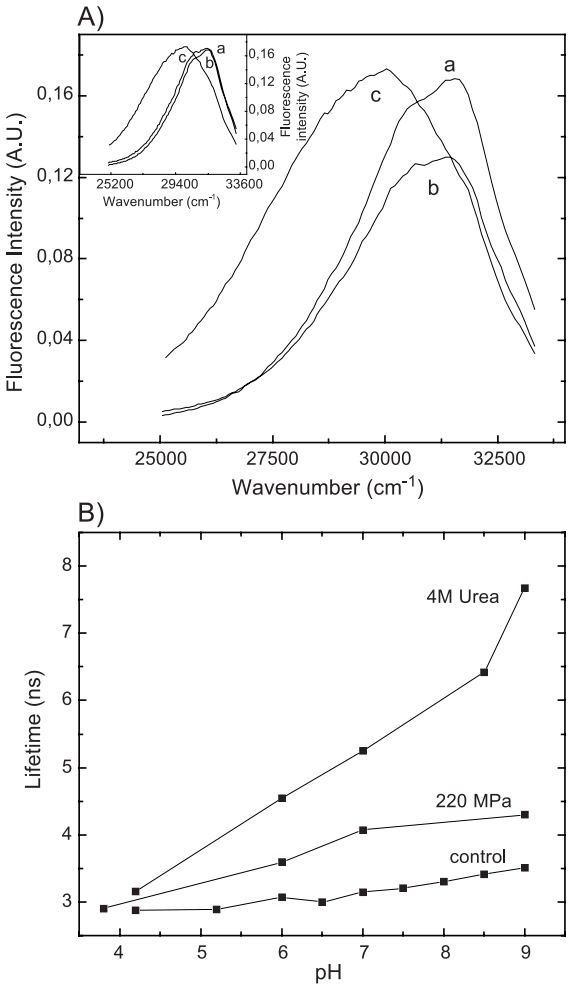

Fig. 6. (A) Effect of pH on the fluorescence emission spectrum at 220 MPa and pH 9.0 (a), at atmospheric pressure and pH 4.2 (b) and at atmospheric pressure, pH 7.5, in the presence of 4 M urea (c). The excitation and emission wavelengths were 285 and 300–400 nm, respectively. Inset: Fluorescence spectra normalized by the maximum intensity. (B) Effect of pH on the lifetime of TMV tryptophans at atmospheric pressure, at 220 MPa, and in the presence of 4 M urea at atmospheric pressure.

length of exposure of the free subunits to water molecules. This description of the energy and dynamics of high protein aggregates can explain the results obtained here, as well as related findings such as the high degree of association observed during a fast cycle of compression/decompression and the progressive decrease in reversibility as the duration of analysis is increased [35,37]. The results obtained for the energy change of dissociation and for the return to atmospheric conditions after compression indicated that, at high pH and high pressure, these low affinity structures predominated in solution, and that their rate of formation was affected by pH and by the pressure of the sample.

The TMV destabilization with increasing pH appears be related to three sites of electrostatic repulsion, with the involvement of carboxylate groups: Glu50 and Asp77 from one subunit, Glu95and Glu106 from adjacent subunits, and the RNA binding site, in which Asp116 is close to one of the RNA phosphates [38,39]. Culver et al. [40] demonstrated that site-directed mutagenesis of Glu50 and Asp77, in which these amino acids were replaced by Gln and Asn, respectively, resulted in alkaline stabilization and a significant loss of infectivity. In this case, most of the proton contribution for the stoichiometry observed (0.584 mol of H^+/mol of TMV subunit) probably came from these three groups.

The ΔV values obtained during pressure dissociation indicated a heterogeneous behavior, with a reduction in the absolute values from -49.7 to -21.7 ml/mol of TMV subunit as the pH increased from 3.8 to 9.0. The signal and magnitude of the volume changes in response to pressure in biological processes have been extensively discussed [41,42]. For most proteins analyzed at low and moderate temperatures, the volume change is negative [43] and the magnitude of the ΔV values is related to the protein's susceptibility to compression [44–46]. A comparison of several dimeric proteins has shown a relative increase in the volume change per mass of protein in smaller dimers. This phenomenon can be explained by a relatively higher number of buried amino acids being exposed to the solvent upon dissociation [47]. The decrease in volume during dissociation can be attributed to: (1) the disruption of salt bridges and consequent hydration, leading to organization of the solvent (electrostriction): (2) the exposure of nonpolar and polar residues followed by hydration: and (3) the solvent occupation of free spaces corresponding to imperfect protein packing [48]. The results obtained here for TMV dissociation at different pH values indicate that a rise in pH may increase the exposure of sites containing charged groups and polar and hydrophobic residues, and may expose buried cavities previously involved in solvent organization and that were filled with solvent. This would reduce the value of ΔV for dissociation. A similar dependence of ΔV values on pH has also been observed for the unfolding of RNase A [49] and for apocytochrome b562 [50], with negative values at 293 K changing from -97 ml/mol at pH 3.92 to -60 ml/mol at pH 10.

Analysis of the ΔV values obtained indicated that, at low pH, a more constrained viral structure predominated in solution because the absolute values for the volume change of dissociation were higher. At more alkaline pH, weakening of the protein interactions allowed further replacement of water molecules in the viral structure and reduced the volume change of dissociation. A similar phenomenon involving a decrease in ΔV with TMV dissociation in increasing concentrations of urea has already been described [25].

The denaturation of viral solutions by hydrostatic pressure up to 200 MPa is not usual. Rotaviruses, for instance, showed no detectable denaturation at high pressure but underwent significant inactivation in a few minutes [51]. However, the presence of urea, even at a low concentration (1.0 M), caused important denaturation. Additional experiments done using the bacteriophage R17 showed a very low

red shift with a pressure increase from 0.1 to 250 MPa, corresponding to 150 cm^{-1}, whereas the presence of urea increased the red shift by pressure to 1000 cm^{-1}. The fluorescence emission spectra for the effect of pH on TMV assembly showed a similar behavior to that observed for the pressure effect. Thus, increasing the pH of the solution facilitated protein dissociation over the pH range analyzed but was unable to produce a significant amount of denaturated structures in the absence of urea. The fluorescence emission spectrum data indicated a similar polarity for tryptophan in the associated and dissociated forms at any pH. In contrast, urea caused a significant red shift in the spectrum, indicating greater polarity.

Analysis of the tryptophan lifetime has been used to study the amino acid environment and the effects of the RNA molecule on the stability of viral particles [52]. These authors compared the middle and bottom components of cowpea mosaic virus, isolated by centrifugation, with the top component formed by empty capsids (and therefore, RNA-free). The tryptophan lifetimes were shorter in the presence of RNA (1.8 and 2.8 ns for the middle and bottom purified components, respectively), while for the RNA-free top component, the lifetime was larger (4.2 ns). These results suggested a reduction in the overall dynamics of the virus particle mediated by the RNA molecule particles [52]. Analogously, the present investigation detected an important pH-mediated modulation of TMV stability. Thus, the observed reduction in lifetime decay at low pH values suggested that the increase in external proton concentration reduced the overall dynamics of the viruses and increased viral stability by simultaneously reinforcing the protein–protein and protein–RNA interactions.

Because the initial evidence for the involvement of protons in the assembly of TMV subunits reported by Sreenivasaya and Pirie [53], many efforts have been made to provide a plausible explanation of the mechanisms involved in this process and their regulation. The approach used here to obtain the average number of protons involved in viral dissociation provides crucial information concerning the role of this effector in virus uncoating. The importance of these results arises fundamentally from the diversity of biological processes that use this effector as a common ion in more than one reaction step. This diversity allows the relative energy states or formation of different protein structures in solution to be modulated by changes in pH, depending on the number of protons involved in each step of the reaction.

The evidence that pH modulates dissociation by high pressure without significantly modifying the dissociated protein structure suggests that ideal conditions for virus inactivation by pressure should be determined in order to improve their immunogenicity and the efficiency of inactivation. The investigation of pressure-mediated inactivation in even more complexes viruses has revealed a series of detailed molecular events. Recent studies of vesicular stomatitis virus, a membrane-enveloped virus, using fluorescence microscopy have shown that pressurized viral particles retain their fusogenic properties with the cell membrane without causing infection [54]. This observation suggests a mechanism of inactivation by pressure. The present results reinforce the expectations in this field and suggest that pressure-inactivation can be a powerful tool for producing antiviral vaccines, for sterilization and for studying the properties of proteins during aggregation and denaturation processes.

Acknowledgements

The authors thank Valdiney A. Pimenta, Jarbas J.R. Rohwedder and Carlos E.S. Luz for automating the pressure system, and Jerson L. Silva and Stephen Hyslop for their helpful discussions. This work was supported by Fundação de Amparo à Pesquisa do Estado de São Paulo (FAPESP), Conselho Nacional de Desenvolvimento Científico e Tecnológico (CNPq), Fundo de Apoio ao Ensino e à Pesquisa–Universidade Estadual de Campinas (FAEP–UNICAMP) and Coordenaç ão de Aperfeiç oamento de Pessoal de Nível Superior (CAPES).

References

[1] K. Namba, G.J. Stubbs, Structure of tobacco mosaic virus at 3.6 Å resolution: implications for assembly, Science 231 (1986) 1401–1406.
[2] D.R. Turner, L.E. Joyce, P.J.G. Butler, The tobacco mosaic virus assembly origin RNA functional characteristics defined by directed mutagenesis, J. Mol. Biol. 203 (1988) 531–547.
[3] X.J. Wu, J. Shaw, Bidirectional uncoating of the genomic RNA of a helical virus, Proc. Natl. Acad. Sci. U. S. A. 93 (1996) 2981–2984.
[4] G. Schramm, G. Schumacher, W. Zillig, Über die struktur des tabakmosaikvirus: III. Der zerfall in alkalischer losung, Z. Naturforsch. 10 (1955) 481–492.
[5] W.F. Harrington, H.K. Schachman, Studies on the alkaline degradation of tobacco mosaic virus: I. Ultracentrifugal analysis, Arch. Biochem. Biophys. 65 (1956) 278–295.
[6] R.N. Perham, Sucrose density gradient analysis of alkaline degradation of tobacco mosaic virus, J. Mol. Biol. 45 (1969) 439–441.
[7] R.N. Perham, T.M.A. Wilson, Polarity of stripping of coat protein subunits from RNA in tobacco mosaic virus under alkaline conditions, FEBS Lett. 62 (1976) 11–15.
[8] T. Ohno, Y. Okada, Polarity of stripping of tobacco mosaic virus by alkali and sodium dodecyl sulfate, Virology 76 (1977) 429–432.
[9] C.A. Powell, Effect of cations on alkaline dissociation of tobacco mosaic virus, Virology 64 (1975) 75–85.
[10] R.N. Perham, T.M.A. Wilson, Characterization of intermediates formed during disassembly of tobacco mosaic virus at alkaline pH, Virology 84 (1978) 293–302.
[11] R. Hogue, A. Asselin, Study of tobacco mosaic virus in vitro disassembly by sucrose density gradient centrifugation and agarose gel electrophoresis, Can. J. Bot. 62 (1984) 457–462.
[12] L.E. Pelcher, M.C. Halasa, Comparative study of the alkaline disassembly of 2 strains of tobacco mosaic virus, Virology 98 (1979) 489–492.
[13] R.A.F. Shalaby, M.A. Lauffer, Hydrogen ion uptake upon tobacco mosaic virus protein polymerization, J. Mol. Biol. 116 (1977) 709–725.

[14] T.M. Schuster, R.B. Scheele, M.L. Adams, S.J. Shire, J.J. Steckert, M. Potschka, Studies on the mechanism of assembly of tobacco mosaic virus, Biophys. J. 32 (1980) 313–329.
[15] R.A. Shalaby, C.L. Stevens, M.A. Lauffer, Ultracentrifugation studies on early stage polymerization of tobacco mosaic virus protein, Arch. Biochem. Biophys. 218 (1982) 384–401.
[16] L.E. Blowers, T.M.A. Wilson, The effect of urea on tobacco mosaic virus polarity of disassembly, J. Gen. Virol. 61 (1982) 137–141.
[17] A.T. Da Poian, J.E. Johnson, J.L. Silva, Differences in pressure stability of the three components of cowpea mosaic virus: implications for virus assembly and disassembly, Biochemistry 33 (1994) 8339–8346.
[18] T. Mesh, R. Kiyama, T. Ohno, Y. Okada, Nucleotide sequence of the coat protein cistron and the 3′ noncoding region of cucumber green mottle mosaic virus (watermelons strain) RNA, Virology 127 (1983) 54–64.
[19] M. Mougel, F. Eyermann, E. Westhof, P. Romby, A. Expert-Bezancon, J.P. Ebel, B. Ehresmann, C. Ehresmann, Binding of *Escherichia coli* ribosomal protein S8 to 16 S rRNA. A model for the interaction and the tertiary structure of the RNA binding site, J. Mol. Biol. 198 (1987) 91–107.
[20] A.T. Da Poian, A.C. Oliveira, J.L. Silva, Cold denaturation of an icosahedral virus: the role of entropy in virus assembly, Biochemistry 34 (1995) 2672–2677.
[21] L.C. Gaspar, J.E. Johnson, J.L. Silva, A.T. Da Poian, Partially folded states of the capsid protein of cowpea severe mosaic virus in the disassembly pathway, J. Mol. Biol. 273 (1997) 456–466.
[22] D. Zimmern, P.J.G. Butler, Isolation of tobacco mosaic virus RNA fragments containing origin for viral assembly, Cell 11 (1977) 455–462.
[23] P.J.G. Butler, Self assembly of tobacco mosaic virus particle: the role of an intermediate aggregate in generating both specificity and speed, Philos. Trans. R. Soc. Lond., B 354 (1999) 537–550.
[24] A. Klug, The tobacco mosaic virus particle: structure and assembly, Philos. Trans. R. Soc. Lond., B 354 (1999) 531–535.
[25] C.F.S. Bonafe, C.M.R. Vital, R.C.B. Telles, M.C. Gonçalves, M.S.A. Matsuura, F.B.T. Pessine, D.R.C. Freitas, J. Vega, Tobacco mosaic virus disassembly by high hydrostatic pressure in combination with urea and low temperature, Biochemistry 37 (1998) 11097–11105.
[26] R.C. Neuman Jr., W. Kauzmann, A. Zipp, Pressure dependence of weak acid ionization in aqueous buffers, J. Phys. Chem. 77 (1973) 2687–2691.
[27] A. Asselin, M. Zaitlin, Characterization of a second protein associated with virion of tobacco mosaic virus, Virology 91 (1978) 173–181.
[28] A.A. Paladini, G. Weber, Absolute measurements of fluorescence polarization at high pressures, Rev. Sci. Instrum. 52 (1981) 419–427.
[29] C. Tanford, Physical Chemistry of Macromolecules, Wiley, New York, 1961.
[30] J.L. Silva, M.S. Villas-Boas, C.F.S. Bonafe, N.C. Meirelles, Anomalous pressure dissociation of large protein aggregates. Lack of concentration dependence and irreversibility at extreme degrees of dissociation of extracellular hemoglobin, J. Biol. Chem. 264 (1989) 15863–15868.
[31] J.L. Silva, G. Weber, Pressure-induced dissociation of Brome mosaic virus, J. Mol. Biol. 199 (1988) 149–159.
[32] A.H. Chu, B.W. Turner, G.K. Ackers, Effect of protons on the oxygenation linked subunit assembly in human hemoglobin, Biochemistry 23 (1984) 604–617.
[33] K. Ruan, G. Weber, Hysteresis and conformational drift of pressure-dissociated glyceraldehydephosphate dehydrogenase, Biochemistry 28 (1989) 2144–2153.
[34] L. Erijman, G. Weber, Oligomeric protein associations: transition from stochastic to deterministic equilibrium, Biochemistry 30 (1991) 1595–1599.
[35] C.F.S. Bonafe, J.R.V. Araujo, J.L. Silva, Intermediate states of assembly in the dissociation of gastropod hemocyanin by hydrostatic pressure, Biochemistry 33 (1994) 2651–2659.
[36] C.F.S. Bonafe, M.S. Villas-Boas, M.C. Suarez, J.L. Silva, Reassembly of a large multisubunit protein promoted by nonprotein factors. Effect of calcium and glycerol on the reassociation of extracellular hemoglobin, J. Biol. Chem. 266 (1991) 13210–13216.
[37] G. Weber, Phenomenological description of the association of protein subunits subjected to conformational drift. Effect of dilution and of hydrostatic pressure, Biochemistry 25 (1986) 3626–3631.
[38] K. Namba, R. Pattanayek, G. Stubbs, Visualization of protein–nucleic acid interactions in a virus. Refined structure of intact tobacco mosaic virus at 2.9-A resolution by X-ray fiber diffraction, J. Mol. Biol. 208 (1989) 307–325.
[39] G. Stubbs, Tobacco mosaic virus particle structure and the initiation of disassembly, Philos. Trans. R. Soc. Lond., B 354 (1999) 551–557.
[40] J.N. Culver, W.O. Dawson, K. Plonk, G. Stubbs, Site directed mutagenesis confirms the involvement of carboxylate groups in the disassembly of tobacco mosaic virus, Virology 206 (1995) 724–730.
[41] W. Kauzmann, Protein stabilization. Thermodynamics of unfolding, Nature 325 (1987) 763–764.
[42] K.A. Dill, Dominant forces in protein folding, Biochemistry 29 (1990) 7133–7155.
[43] C.A. Royer, Revisiting volume changes in pressure-induced protein unfolding, Biochim. Biophys. Acta 159 (2002) 201–209.
[44] C.E. Kundrot, F.M. Richards, Crystal structure of hen egg white lysozyme at a hydrostatic pressure of 1000 atmospheres, J. Mol. Biol. 193 (1987) 157–170.
[45] K. Akasaka, T. Tesuka, H. Yamada, Pressure-induced changes in the folded structure of lysozyme, J. Mol. Biol. 271 (1997) 671–678.
[46] K. Akasaka, H. Li, Low-lying excited states of proteins revealed from nonlinear pressure shifts in ^{1}H and ^{15}N NMR, Biochemistry 40 (2001) 8665–8671.
[47] J.L. Silva, G. Weber, Pressure stability of proteins, Adv. Rev. Phys. Chem. 44 (1993) 89–113.
[48] J.L. Silva, D. Foguel, C.A. Royer, Pressure provides new insights into protein folding, dynamics and structure, Trends Biochem. Sci. 26 (2001) 612–618.
[49] J.F. Brandts, R.J. Oliveira, C. Westort, Thermodynamics of protein denaturation. Effect of pressure on denaturation of ribonuclease A, Biochemistry 4 (1970) 1038–1047.
[50] E.J. Fuents, A.J. Wand, Local dynamics and stability of apocytochrome b562 examined by hydrogen exchange, Biochemistry 37 (1998) 3687–3698.
[51] L. Pontes, Y. Cordeiro, V. Giongo, M.S. Villas-Boas, A. Barreto, J.R.V. Araujo, J.L. Silva, Pressure-induced formation of inactive triple-shelled rotavirus particles is associated with changes in the spike protein, J. Mol. Biol. 307 (2001) 1171–1179.
[52] A.T. Da Poian, J.E. Johnson, J.L. Silva, Protein–RNA interactions and virus stability as probed by the dynamics of tryptophan side chains, J. Biol. Chem. 277 (2002) 47596–47602.
[53] M. Sreenivasaya, N.W. Pirie, CCXXII. The disintegration of tobacco mosaic virus preparations with sodium dodecyl sulphate, Biochem. J. 32 (1938) 1707–1710.
[54] A.M.O. Gomes, A.S. Pinheiro, C.F.S. Bonafe, J.L. Silva, Pressure-induced fusogenic conformation of vesicular stomatitis virus glycoprotein, Biochemistry 42 (2003) 5540–5546.